BUHEP-95-19
hep-ph/9506427

Limits on Non-Commuting Extended Technicolor

R.S. Chivukula*, E.H. Simmons, and J. Terning
Department of Physics, Boston University,
590 Commonwealth Ave., Boston MA 02215

June 26, 1995

Abstract

Using precision electroweak data, we put limits on non-commuting extended technicolor models. We conclude that these models are viable only if the ETC-interactions are strong. Interestingly, these models predict a pattern of deviations from the standard model which can fit the data significantly better than the standard model does, even after taking into account the extra parameters involved.

*e-mail addresses: sekhar@bu.edu, simmons@bu.edu, terning@calvin.bu.edu

1 Introduction

There continue to be several small discrepancies between precision electroweak measurements and the predictions of the standard model [1, 2, 3]. The most interesting is associated with the ratio of the Z decay widths to $b\overline{b}$ and to all hadrons (R_b). In addition if $\alpha_s(M_Z) \approx 0.115$, as suggested by recent lattice results [4] and deep-inelastic scattering [1, 5], there are also potentially significant deviations in the ratios of the hadronic to leptonic widths. If new physics which increased R_b were present, a better fit to precision electroweak data would be obtained with a value of $\alpha_s(M_Z)$ comparable to the value quoted above [6].

Recently it was shown that in non-commuting extended technicolor (ETC) models, in which in which the ETC interactions [7] do not commute with the $SU(2)_L$ interactions of the standard model (i.e., in which $SU(2)_L$ is partially embedded in the ETC gauge group), R_b could exceed the standard model value [8]. In that discussion, we assumed that only the (t, b) doublet had non-commuting ETC couplings suppressed by a scale low enough to provide observable consequences at present machines. From the point of view of anomaly cancellation, it is much more economical to assume that the entire third generation has the same non-commuting ETC interactions. Such a scheme implies that the electroweak interactions of the τ and ν_τ will also exhibit interesting deviations.

In this paper we will use the wealth of precision electroweak data to place constraints on such non-commuting ETC family models. After reviewing non-commuting ETC models, we discuss the deviations from the standard model that this new physics would produce. We discuss the amount of fine-tuning these models require to accommodate the top quark mass and to agree with the precision electroweak data. We conclude that these models predict a pattern of deviations from the standard model which can fit the data significantly better than the standard model does, even after taking into account the extra parameters involved.

2 Non-Commuting Extended Technicolor

2.1 Gauge Symmetry-Breaking Pattern

The pattern of gauge symmetry breaking that is required in non-commuting ETC models is more complicated than that in commuting ETC models; it generally involves three scales (rather than just two) to provide masses for one family of ordinary fermions. The required pattern of breaking is as follows:

$$\begin{array}{c} G_{ETC} \otimes SU(2)_{light} \otimes U(1)' \\ \downarrow \quad f \\ G_{TC} \otimes SU(2)_{heavy} \otimes SU(2)_{light} \otimes U(1)_Y \\ \downarrow \quad u \\ G_{TC} \otimes SU(2)_L \otimes U(1)_Y \end{array}$$

$$\downarrow \quad v$$
$$G_{TC} \otimes U(1)_{em},$$

The ETC gauge group is broken to technicolor and an $SU(2)_{heavy}$ subgroup at the scale f. The $SU(2)_{heavy}$ gauge group is effectively the weak gauge group for the third generation in these non-commuting ETC models, while the $SU(2)_{light}$ is the weak gauge group for the two light generations. The two $SU(2)$'s are mixed (i.e. they break down to a diagonal $SU(2)_L$ subgroup) at the scale u. Finally the electroweak gauge symmetry breaking is accomplished at the scale v, as is standard in technicolor theories.

The two simplest possibilities for the $SU(2)_{heavy} \times SU(2)_{light}$ transformation properties of the order parameters that produce the correct combination of mixing and breaking of these gauge groups are:

$$\langle\varphi\rangle \sim (2,1)_{1/2}, \quad \langle\sigma\rangle \sim (2,2)_0 \ , \qquad \text{“heavy case”} \ , \tag{2.1}$$

and

$$\langle\varphi\rangle \sim (1,2)_{1/2}, \quad \langle\sigma\rangle \sim (2,2)_0 \ , \qquad \text{“light case”} \ . \tag{2.2}$$

Here the order parameter $\langle\varphi\rangle$ is responsible for breaking $SU(2)_L$ while $\langle\sigma\rangle$ mixes $SU(2)_{heavy}$ with $SU(2)_{light}$. We refer to these two possibilities as “heavy” and “light” according to whether $\langle\varphi\rangle$ transforms non-trivially under $SU(2)_{heavy}$ or $SU(2)_{light}$.

The heavy case, in which $\langle\varphi\rangle$ couples to the heavy group, is the choice made in [8], and corresponds to the case in which the technifermion condensation responsible for providing mass for the third generation of quarks and leptons is also responsible for the bulk of electroweak symmetry breaking (as measured by the contribution made to the W and Z masses). The light case, in which $\langle\varphi\rangle$ couples to the light group, corresponds to the opposite scenario: here the physics responsible for providing mass for the third generation *does not* provide the bulk of electroweak symmetry breaking. While this light case is counter-intuitive (after all, the third generation is the heaviest!), it may in fact provide a resolution to the issue of how large isospin breaking can exist in the fermion mass spectrum (and, hence, the technifermion spectrum) without leaking into the W and Z masses. This is essentially what happens in multiscale models [11, 12] and in top-color assisted technicolor [13]. Such hierarchies of technifermion masses are also useful for reducing the predicted value of S in technicolor models[1] [15].

2.2 Top Quark Mass Generation

In ETC models the top quark mass [7] is generated by four-fermion operators induced by ETC gauge boson exchange. In non-commuting ETC models, the left-handed third generation quarks and right-handed technifermions, $\psi_L = (t,b)_L$ and

[1] Recently the experimental upper bound on S has been relaxed, so that substantially positive values of S are allowed. Ref. [14] gives $S < 0.4$ at the 95% confidence level.

$T_R = (U, D)_R$, are doublets under $SU(2)_{heavy}$ while the left-handed technifermions are $SU(2)_{heavy}$ singlets, and these operators may be written as

$$\mathcal{L}_{4f} = -\frac{2}{f^2}\left(\xi\bar{\psi}_L\gamma^\mu U_L + \frac{1}{\xi}\bar{t}_R\gamma^\mu T_R\right)\left(\xi\bar{U}_L\gamma_\mu\psi_L + \frac{1}{\xi}\bar{T}_R\gamma_\mu t_R\right) \ , \tag{2.3}$$

where ξ is a model-dependent Clebsch. When the technifermions condense the LR cross-terms in the operator (2.3) produce a top quark mass. In strong-ETC models, i.e. models in which the ETC coupling is fine-tuned to be close to the critical value necessary for the ETC interactions to produce chiral symmetry breaking, the LR-interactions become enhanced. Physically, this is due to the presence of a composite scalar [10] which is light compared to f and communicates electroweak symmetry breaking to the top quark.

Whether or not the ETC interactions are strong, we can write the top quark mass as [7]

$$m_t \approx \frac{g^2 4\pi f_Q^3}{M^2} \ , \tag{2.4}$$

where the numerator contains an estimate of the technifermion condensate (using dimensional analysis [9]), and f_Q is the Goldstone boson decay constant associated with the technifermions which feed down a mass to the top quark. In the heavy case the technifermions responsible for giving rise to the third-generation masses also provide the bulk of the W and Z masses, and we expect $f_Q \approx 125$ GeV (which, for $m_t \approx 175$ GeV, implies $M/g \approx 375$ GeV). Even in the light case there must be some $SU(2)_{heavy}$ breaking vev, that is $f_Q \neq 0$, in order to give the top-quark a mass. However, it is unreasonable to expect that M/g can be tuned to be smaller than f_Q and equation (2.4) implies the lower bound $f_Q > 14$ GeV.

In an ETC theory with no fine-tuning, M represents the mass of the ETC gauge boson, which is related to f by

$$M = \frac{gf}{2} \ , \tag{2.5}$$

where g is the ETC gauge coupling. In strong-ETC theories [16], g^2 is the product of the scalar couplings to the top quark and the technifermions and M is the mass of the light composite scalar [10]. In the context of these theories, the "accuracy" with which the ETC gauge coupling must be adjusted is approximately equal to the ratio of M^2/g^2 to its naive value, $f^2/4$. That is, a rough measure of fine-tuning required is

$$\frac{4M^2}{g^2 f^2} \approx \frac{8\pi f_Q^3}{m_t f^2}. \tag{2.6}$$

2.3 Shifts in Z Couplings

As discussed in Ref. [8], the LL (and, in principle, RR) terms in the operator (2.3) produce a shift in the $Zb\overline{b}$ coupling:

$$\delta g_L^b = -\frac{\xi^2 f_Q^2}{2f^2} \ . \tag{2.7}$$

(For convenience, we have factored out $e/\sin\theta\cos\theta$ from all the Z couplings.) The difference between the scenario proposed in Ref. [8] and that proposed here is that here the entire third family couples to the same ETC gauge bosons, so there will also be corrections for the τ and ν_τ couplings:

$$\delta g_L^\tau = \delta g_L^{\nu_\tau} = -\frac{\xi^2 f_L^2}{2f^2} \ , \tag{2.8}$$

where we have allowed for the possibility that the technilepton condensate is different from the techniquark condensate (i.e. $f_Q \neq f_L$).

From the analysis given in Ref. [8], we see that *in the absence of fine-tuning* we expect the four-fermion operator (2.3) to induce corrections to the third-generation couplings of the order of a few percent. Our fits to precision electroweak measurements will allow us to put a lower bound on the size of f. We will translate this, using equation (2.6) into an estimate of the amount of fine-tuning required to produce a viable theory.

3 Weak Boson Mixing: Heavy Case

The remaining corrections come from weak gauge boson mixing[2]. The $U(1)_{em}$ to which the electroweak group breaks is generated by

$$Q = T_{3l} + T_{3h} + Y \ . \tag{3.1}$$

The photon eigenstate can be written in terms of two weak mixing angles,

$$A^\mu = \sin\theta\sin\phi\, W_{3l}^\mu + \sin\theta\cos\phi\, W_{3h}^\mu + \cos\theta X^\mu \ , \tag{3.2}$$

where θ is the weak angle and ϕ is an additional mixing angle. Equations (3.1) and (3.2) imply that the gauge couplings are

$$\begin{aligned} g_l &= \frac{e}{s\sin\theta} \ , \\ g_h &= \frac{e}{c\sin\theta} \ , \\ g' &= \frac{e}{\cos\theta} \ , \end{aligned} \tag{3.3}$$

[2] The discussion of gauge boson mixing presented in this section and the next follows the discussion of mixing in the un-unified standard model given in Refs. [17, 18].

where $s \equiv \sin\phi$ and $c \equiv \cos\phi$.

Consider the low energy weak interactions in the four-fermion approximation. For the charged-currents, if we combine the left-handed light and heavy fermion currents into the vector $J^\dagger = (j_l, j_h)$, then the four-fermion interactions are $2\, J^\dagger\, V^{-2}\, J$ where

$$V^{-2} = \frac{1}{u^2\, v^2} \begin{pmatrix} u^2+v^2 & u^2 \\ u^2 & u^2 \end{pmatrix} . \tag{3.4}$$

Retaining the standard relation between the μ decay rate and G_F requires

$$\sqrt{2} G_F = \frac{1}{v^2} + \frac{1}{u^2} . \tag{3.5}$$

Hence the charged-current four-fermion weak interactions can be written

$$2\sqrt{2} G_F\, (j_l + j_h)^2 - \frac{2}{u^2}(j_h^2 + 2 j_l j_h\,) . \tag{3.6}$$

The extra $j_l j_h$ term will affect the weak decays of third-generation fermions. For example, the effect on the tau decay rate to muons is illustrated in Appendix A (equation (A.22)). The low-energy neutral-current interactions can be obtained similarly in terms of j_{em}, the electromagnetic fermion current, and $j_{3l,3h}$, the left-handed T_3 currents of light- and heavy-charged fermions. Applying (3.5) gives

$$\begin{aligned} & 2\sqrt{2} G_F\, (j_{3l} + j_{3h} - \, j_{em} \sin^2\theta)^2 \qquad (3.7) \\ - \quad & \frac{2}{u^2} \left[-j_{3h}^2 - 2 j_{3l} j_{3h} + \sin^2\theta \; j_{em}(2 j_{3h} + 2 j_{3l} c^2 + j_{em} \sin^2\theta (s^4 - 1)) \right] . \end{aligned}$$

Note that the extra neutral-current interactions involving third generation fermions are suppressed only by v^2/u^2, whereas those involving only charged first and second generation fermions are additionally suppressed by mixing angles.

It is convenient to discuss the mass eigenstates in the rotated basis

$$\begin{aligned} W_1^\pm &= s\, W_l^\pm + c\, W_h^\pm , & (3.8) \\ W_2^\pm &= c\, W_l^\pm - s\, W_h^\pm , & (3.9) \\ Z_1 &= \cos\theta\, (s\, W_{3l} + c\, W_{3h}) - \sin\theta\, X , & (3.10) \\ Z_2 &= c\, W_{3l} - s\, W_{3h} , & (3.11) \end{aligned}$$

in which the gauge covariant derivatives separate neatly into standard and non-standard pieces

$$\begin{aligned} D^\mu &= \partial^\mu + ig \left(T_l^\pm + T_h^\pm \right) W_1^{\pm\mu} + ig \left(\frac{c}{s} T_l^\pm - \frac{s}{c} T_h^\pm \right) W_2^{\pm\mu} \\ &\quad + i \frac{g}{\cos\theta} \left(T_{3l} + T_{3h} - \sin^2\theta\, Q \right) Z_1^\mu + ig \left(\frac{c}{s} T_{3l} - \frac{s}{c} T_{3h} \right) Z_2^\mu . \end{aligned} \tag{3.12}$$

where $g \equiv \frac{e}{\sin\theta}$. The breaking of $SU(2)_L$ results in mixing of Z_1 and Z_2, as well as a mixing of $W_1^\pm$ and $W_2^\pm$. The mass-squared matrix for the Z_1 and Z_2 is:

$$M_Z^2 = \left(\frac{ev}{2\sin\theta}\right)^2 \begin{pmatrix} \frac{1}{\cos^2\theta} & \frac{-s}{c\cos\theta} \\ \frac{-s}{c\cos\theta} & \frac{x}{s^2c^2} + \frac{s^2}{c^2} \end{pmatrix}, \tag{3.13}$$

where $x = u^2/v^2$. The mass-squared matrix for W_1 and W_2 is obtained by setting $\cos\theta = 1$ in the above matrix.

Diagonalizing the W and Z mass matrices in the limit of large x and taking into account the value of G_F given in equation (3.5), we find for the lightest eigenstates

$$M_W^2 \approx \left(\frac{\pi\alpha_{em}}{\sqrt{2}G_F\sin^2\theta}\right)\left(1 + \frac{1}{x}(1-s^4)\right), \tag{3.14}$$

$$W^L \approx W_1 + \frac{cs^3}{x} W_2 \tag{3.15}$$

and

$$M_Z^2 \approx \left(\frac{\pi\alpha_{em}}{\sqrt{2}G_F\sin^2\theta\cos^2\theta}\right)\left(1 + \frac{1}{x}(1-s^4)\right), \tag{3.16}$$

$$Z^L \approx Z_1 + \frac{cs^3}{x\cos\theta} Z_2 \ . \tag{3.17}$$

Note that to this order in $1/x$, the custodial isospin relation for the W and Z masses is preserved.

Thus, weak gauge boson mixing produces a shift from the standard model Z couplings:

$$\delta g_L^f = \frac{cs^3}{x}\left(\frac{c}{s} T_{3l} - \frac{s}{c} T_{3h}\right) \ . \tag{3.18}$$

Furthermore, the relationship between M_Z, G_F, and $\sin^2\theta$ given in equation (3.16) differs from that in the standard model[3]. Both effects must be taken into account in comparing the predictions of this model with those of the standard model.

The result of all these corrections is that the predicted values of many electroweak observables are altered from those given by the standard model[4] [18, 19]. For example, we find that the W mass is changed as follows:

$$M_W = (M_W)_{SM}\left(1 - 0.213\left(1-s^4\right)\frac{1}{x}\right) \ . \tag{3.19}$$

Likewise, one finds that the total width of the Z becomes:

$$\begin{aligned} \Gamma_Z \ &= \ (\Gamma_Z)_{SM}\Big(1 - 0.707\delta g_L^b - 0.144\delta g_L^\tau + 0.268\delta g_L^{\nu_\tau} \\ &\qquad + \left(1.693s^2c^2 - 0.559s^4 - 1.350\left(1-s^4\right)\right)\frac{1}{x}\Big) \ . \end{aligned} \tag{3.20}$$

[3] In the notation of Ref. [19], we can account for this effect by the replacement $\Delta_e + \Delta_\mu = (1-s^4)/x$.

[4] We are using $\alpha_{em}(M_Z)$, G_F, and M_Z as the tree-level inputs.

The full list of changes to the electroweak observables that we use in our fits for the heavy case non-commuting ETC model appears in Appendix A.

Finally, we can combine previously obtained expressions for the masses of the heavy W boson and the top quark to constrain x. The analysis of the mass matrix shows that the mass of the heavy W gauge boson is

$$M_W^H \approx \frac{\sqrt{x}}{sc} M_W \ . \tag{3.21}$$

If we combine this equation with the estimate of the top mass given in equation (2.4) , we find

$$M_W^H \approx \frac{210 \text{ GeV}}{sc} \left(\frac{175 \text{ GeV}}{m_t}\right)^{\frac{1}{2}} \left(\frac{3 f_Q}{v}\right)^{\frac{3}{2}} \left(\frac{u}{f}\right) \ . \tag{3.22}$$

The last two factors on the right hand side of this equation are written so that they are of the order of, or less than, unity when there is no fine-tuning of the ETC interactions. Therefore, we find

$$M_W^H \leq \frac{210 \text{ GeV}}{sc} \tag{3.23}$$

which, together with (3.21), implies that

$$x \leq 6.9 \tag{3.24}$$

assuming the absence of strong-ETC fine-tuning or an alternative mechanism for generating the top mass. As we will see in section 5, these bounds will not be satisfied: some fine-tuning will be required.

4 Weak Boson Mixing: Light Case

The four-fermion operators induced by ETC gauge boson exchange produce the same corrections in both the heavy and the light case. The differences between the two cases arises in the low energy weak interactions and in how the breaking of $SU(2)_L$ mixes Z_1 and Z_2, and $W_1^{\pm}$ and $W_2^{\pm}$. In the light case, retaining the standard relation between the μ decay rate and G_F yields

$$\sqrt{2} G_F = \frac{1}{v^2} \ . \tag{4.1}$$

The charged-current four-fermion weak interactions are of the form

$$2\sqrt{2} G_F \left(j_l + j_h\right)^2 + \frac{2}{u^2} j_h^2 \tag{4.2}$$

while the low-energy neutral-current interactions can be written

$$2\sqrt{2}G_F\,(j_{3l}+j_{3h}-\,j_{em}\sin^2\theta)^2+\frac{2}{u^2}\,(j_{3h}-s^2\sin^2\theta j_{em})^2\ . \tag{4.3}$$

Note that this time the charged-current weak interactions contain no new $j_l j_h$ term, so that the weak decays of third-generation fermions will not be altered from their standard rates (see e.g. Appendix B, equation (B.22)).

An analysis of weak gauge boson mixing shows that the mass-squared matrix for the Z_1 and Z_2 is:

$$M_Z^2=\left(\frac{ev}{2\sin\theta}\right)^2\begin{pmatrix}\frac{1}{\cos^2\theta} & \frac{c}{s\cos\theta}\\ \frac{c}{s\cos\theta} & \frac{x}{s^2c^2}+\frac{c^2}{s^2}\end{pmatrix}. \tag{4.4}$$

The mass-squared matrix for W_1 and W_2 is obtained by setting $\cos\theta=1$ in the above matrix. We again diagonalize the W and Z mass matrices in the limit of large x and find

$$M_W^2\approx\left(\frac{\pi\alpha_{em}}{\sqrt{2}G_F\sin^2\theta}\right)\left(1-\frac{c^4}{x}\right), \tag{4.5}$$

$$W^L\approx W_1-\frac{c^3 s}{x}\,W_2 \tag{4.6}$$

and

$$M_Z^2\approx\left(\frac{\pi\alpha_{em}}{\sqrt{2}G_F\sin^2\theta\cos^2\theta}\right)\left(1-\frac{c^4}{x}\right), \tag{4.7}$$

$$Z^L\approx Z_1-\frac{c^3 s}{x\cos\theta}\,Z_2\ . \tag{4.8}$$

Once again, the custodial isospin relation for the W and Z masses is preserved, to this order in $1/x$.

Thus, in this case the weak gauge boson mixing produces the following shift from the standard model Z couplings:

$$\delta g_L^f=-\frac{c^3 s}{x}\left(\frac{c}{s}\,T_{3l}-\frac{s}{c}\,T_{3h}\right)\ . \tag{4.9}$$

The difference in the relationship between G_F, M_Z, and $\sin^2\theta$ in equation (4.8) and the corresponding relationship in the standard model must also be taken into account[5].

As in the heavy case, the predicted values of electroweak observables are altered from those given by the standard model [18, 19]. For example, we find that the W mass is altered as follows:

$$M_W=(M_W)_{SM}\left(1+0.213\,c^4\frac{1}{x}\right)\ . \tag{4.10}$$

[5]In this case, using the notation of Ref. [19], we can account for the effect by the replacement $\Delta_e+\Delta_\mu=-c^4/x$.

Likewise, one finds that the total width of the Z is changed to:

$$\Gamma_Z = (\Gamma_Z)_{SM} \Big(1 - 0.707\delta g_L^b - 0.144\delta g_L^\tau + 0.268\delta g_L^{\nu_\tau} + \Big(-0.343c^4 + 0.559s^2c^2\Big)\frac{1}{x}\Big) \ . \quad (4.11)$$

The full list of changes to the electroweak observables used in our fits for the light case non-commuting ETC model is given in Appendix B.

5 Comparison with Data

Using the current experimental values of the electroweak observables and the corresponding best-fit *standard model* predictions, we have used the equations given in Appendices A and B to fit the heavy case and light case non-commuting ETC model predictions to the data. Our analysis determines how well each model fits the data, and whether fine-tuning of the ETC interactions is required.

Even before performing multi-variable fits to the precision electroweak data, we can place a constraint on this class of models. We must require that technicolor coupling at the ETC scale, f, not be so strong as to exceed the "critical" value at which technifermion chiral symmetry breaking occurs. If we use the results of the gap-equation analysis of chiral symmetry breaking in the "rainbow" approximation [20] to estimate this value, we find that [8]

$$c^2 > 0.03\left(\frac{N^2-1}{2N}\right) \ , \quad (5.1)$$

where we have assumed that the technifermions form a fundamental representation, N, of an $SU(N)$ technicolor group.

Before describing the details of the fit, we discuss higher-order corrections. Beyond tree-level, the predictions of the standard or non-commuting ETC models depend on the values of $\alpha_s(M_Z)$ and the top-quark mass m_t. Given the success of the standard model, we expect that, for the allowed range of s^2, $1/x$, and the various δg's, the changes in the predicted values of physical observables due to radiative corrections in the standard model or non-commuting ETC models will be approximately the same *for the same values of* $\alpha_s(M_Z)$ *and* m_t.

The best-fit standard model predictions which we use [1] are based on a top quark mass of 173 GeV (taken from a fit to precision electroweak data) which is consistent with the range of masses (176 ± 13 GeV) preferred by CDF and consistent with D0 [22].

The treatment of $\alpha_s(M_Z)$ is more problematic: the LEP determination for $\alpha_s(M_Z)$ comes from a *fit* to electroweak observables *assuming* the validity of the standard model. For this reason it is important [6] to understand how the bounds vary for different values of $\alpha_s(M_Z)$. We present results for bounds on s^2, $1/x$, and

the δg's, both for $\alpha_s(M_Z) = 0.124$ (which is the LEP best-fit value assuming the standard model is correct [1]) and for $\alpha_s(M_Z) = 0.115$ as suggested by recent lattice results [4] and deep-inelastic scattering [1, 5]. To the accuracy to which we work, the α_s dependence of the standard model predictions only appears in the Z partial widths and we use [1]

$$\Gamma_q = \Gamma_q|_{\alpha_s=0} \left(1 + \frac{\alpha_s}{\pi} + 1.409 \left(\frac{\alpha_s}{\pi}\right)^2 - 12.77 \left(\frac{\alpha_s}{\pi}\right)^3\right) \tag{5.2}$$

to obtain the standard model predictions for $\alpha(M_Z) = 0.115$.

We have performed a global fit for the parameters of the non-commuting ETC model (s^2, $1/x$, and the δg's) to all precision electroweak data: the Z line shape, forward backward asymmetries, τ polarization, and left-right asymmetry measured at LEP and SLC; the W mass measured at FNAL and UA2; the electron and neutrino neutral current couplings determined by deep-inelastic scattering; the degree of atomic parity violation measured in Cesium; and the ratio of the decay widths of $\tau \to \mu\nu\bar{\nu}$ and $\mu \to e\nu\bar{\nu}$. Essentially we find that, while both the heavy and light cases provide a better fit to the data than the standard model, the light case can reproduce the data with much smaller gauge boson masses, and hence is of more phenomenological interest.

In Table 1 we compare the predictions of the standard model and the non-commuting ETC model (with particular values of $1/x$ and s^2) with the experimental values. For s^2, we have chosen a value of 0.97 which saturates our bound (5.1), since this conforms to our expectation that the ETC gauge coupling is quite strong. For $1/x$, in the heavy case we show the best fit value of $1/x = 0.0027$ or equivalently $M_W^H = 9$ TeV. The choice of a particular value of $1/x$ for the light case is fairly arbitrary. We do not show the best fit case, since it lies the unphysical region of negative x (the fit gives $1/x = -0.17 \pm 0.75$). However, since the fit is fairly insensitive to the value of $1/x$ (i.e. the uncertainty in $1/x$ is large) there is a substantial range of values for $1/x$ which provide a good fit to the data. For illustration we have chosen the value $1/x = 0.055$ which corresponds to $M_W^H = 2$ TeV.

5.1 The Light Case

We will first discuss the light case in some detail. We have fit the precision electroweak data to the expressions in Appendix B, allowing $s^2, 1/x$, and the δg's to vary. Figure 1 summarizes the fits by displaying the 95% and 68% confidence level lower bounds (solid and dotted lines) on the heavy W mass (M_W^H) for different values of s^2 (using $\alpha_s(M_Z) = 0.115$ as before). The plot was created as follows: for each value of s^2 we fit to the three independent parameters (δg_L^b, $\delta g_L^\tau = \delta g_L^{\nu_\tau}$, and $1/x$); we then found the lower bound on x and translated it into a lower bound on the heavy W mass. Note that for $s^2 > 0.85$, the 95% confidence level allows the heavy W gauge boson to be as light as 400 GeV.

Quantity	Experiment	SM	$\text{ETC}_{\text{heavy}}$	$\text{ETC}_{\text{light}}$
Γ_Z	2.4976 ± 0.0038	2.4923	2.4991	2.5006
R_e	20.86 ± 0.07	20.73	20.84	20.82
R_μ	20.82 ± 0.06	20.73	20.84	20.82
R_τ	20.75 ± 0.07	20.73	20.74	20.73
σ_h	41.49 ± 0.11	41.50	41.48	41.40
R_b	0.2202 ± 0.0020	0.2155	0.2194	0.2188
A_{FB}^e	0.0156 ± 0.0034	0.0160	0.0159	0.0160
A_{FB}^μ	0.0143 ± 0.0021	0.0160	0.0159	0.0160
A_{FB}^τ	0.0230 ± 0.0026	0.0160	0.0164	0.0164
$A_\tau(P_\tau)$	0.143 ± 0.010	0.146	0.150	0.150
$A_e(P_\tau)$	0.135 ± 0.011	0.146	0.146	0.146
A_{FB}^b	0.0967 ± 0.0038	0.1026	0.1026	0.1030
A_{FB}^c	0.0760 ± 0.0091	0.0730	0.0728	0.0730
A_{LR}	0.1637 ± 0.0075	0.1460	0.1457	0.1460
M_W	80.17 ± 0.18	80.34	80.34	80.34
M_W/M_Z	0.8813 ± 0.0041	0.8810	0.8810	0.8810
$g_L^2(\nu N \to \nu X)$	0.3003 ± 0.0039	0.3030	0.3026	0.3030
$g_R^2(\nu N \to \nu X)$	0.0323 ± 0.0033	0.0300	0.0301	0.0300
$g_{eA}(\nu e \to \nu e)$	-0.503 ± 0.018	-0.506	-0.506	-0.506
$g_{eV}(\nu e \to \nu e)$	-0.025 ± 0.019	-0.039	-0.038	-0.039
$Q_W(Cs)$	-71.04 ± 1.81	-72.78	-72.78	-72.78
$R_{\mu\tau}$	0.9970 ± 0.0073	1.0	0.9946	1.0

Table 1: Experimental [1, 2, 21] and predicted values of electroweak observables for the standard model and non-commuting ETC model (heavy and light cases) for $\alpha_s(M_Z) = 0.115$, and $s^2 = 0.97$. For the heavy case $1/x$ is allowed to assume the best-fit value of 0.0027; for the light case, $1/x$ is set to 0.055. The standard model values correspond to the best-fit values (with $m_t = 173$ GeV, $m_{\text{Higgs}} = 300$ GeV) in [1], corrected for the change in $\alpha_s(M_Z)$, and the revised extraction [23] of $\alpha_{em}(M_Z)$.

As mentioned previously, the predictions of the non-commuting ETC model in the light case are given in Table 1. The question remains as to how well this model fits the precision data. The summary of the quality of the fit is given in Table 2. The table shows the fit to the standard model for comparison; as a further benchmark we have included a fit to purely oblique corrections (the S and T parameters) [24]. The percentage quoted in the Table is the probability of obtaining a χ^2 as large or larger than that obtained in the fit, for the given number of degrees of freedom (df), assuming that the model is correct. Thus a small probability corresponds to a poor fit, and a bad model. The $SM + S, T$ fit demonstrates that merely having more parameters is not sufficient to ensure a better fit.

Model	χ^2	df	χ^2/df	probability
SM	33.8	22	1.53	5%
SM+S,T	32.8	20	1.64	4%
$\text{ETC}_{\text{light}}$	22.6	20	1.13	31%

Table 2: The best fits for the standard model, beyond the standard model allowing S and T to vary, and the non-commuting ETC model (light case). The inputs are: $\alpha_s(M_Z) = 0.115$, $1/x = 0.055$, and $s^2 = 0.97$. χ^2 is the sum of the squares of the difference between prediction and experiment, divided by the error.

The best fit values for the shifts in the Z couplings (corresponding to Tables 1 and 2, i.e. the light case with $\alpha_s(M_Z) = 0.115$) are:

$$\begin{aligned} \delta g_L^b &= -0.0035 \pm 0.0015 \\ \delta g_L^\tau &= \delta g_L^{\nu_\tau} = -0.0002 \pm 0.0009 \ . \end{aligned} \tag{5.3}$$

The 90% confidence region for this fit is shown as the solid line in Figure 2. From equation (5.3) and Figure 2 we see that the data prefers a significant shift in the $Zb\overline{b}$ coupling.

Using the values above and equation (2.7) we can obtain a 95% limit on the scale f:

$$f > \xi \cdot 123\,\text{GeV}. \tag{5.4}$$

Using equation (2.6) we see that we require a fine-tuning of the ETC coupling of order:

$$\frac{4M^2}{g^2 f^2} \approx 52\% \left(\frac{f_Q}{30\,\text{GeV}}\right)^3 \left(\frac{123\,\text{GeV}}{f}\right)^2 \left(\frac{175\,\text{GeV}}{m_t}\right). \tag{5.5}$$

From Tables 1 and 2 we see that because the theory accommodates changes in the Z partial widths, the non-commuting ETC model gives a significantly better fit to the experimental data than the standard model does, even after taking into account that in the fitting procedure the non-commuting ETC model has two extra parameters.

Model	χ^2	df	χ^2/df	probability
SM	27.8	21	1.33	15%
SM+S,T	27.7	20	1.38	12%
$\text{ETC}_{\text{light}}$	25.0	20	1.25	20%

Table 3: The best fits for the standard model, beyond the standard model allowing S and T to vary, and the non-commuting ETC model (light case). The inputs are: $\alpha_s(M_Z) = 0.124$, $1/x = 0.055$, and $s^2 = 0.97$.

In particular the non-commuting ETC model predicts values for Γ_Z, R_e, R_μ, R_τ, and R_b that are closer to experiment than those predicted by the standard model.

For comparison we have also performed the fits using $\alpha_s(M_Z) = 0.124$; the quality of the fit is summarized in Table 3. The best fit values for the shifts in the Z couplings (corresponding to Table 3, i.e. the light case with $\alpha_s(M_Z) = 0.124$) are:

$$\begin{aligned} \delta g_L^b &= -0.0013 \pm 0.0015 \\ \delta g_L^\tau &= \delta g_L^{\nu_\tau} = -0.0003 \pm 0.0009 \ . \end{aligned} \tag{5.6}$$

The 90% confidence region for this fit is shown as the dashed line in Figure 2. We find that, while the standard model fit improves for a larger value of $\alpha_s(M_Z)$, the light case of the non-commuting ETC model remains a somewhat better fit.

5.2 The Heavy Case

For the heavy case, we have fit the precision electroweak data to the expressions in Appendix A, allowing s^2, $1/x$ and the δg's to vary. Our results are summarized in Figure 3, which displays the 95% and 68% confidence lower bounds on the heavy W boson (solid and dotted lines) as a function of s^2. For comparison, we show the upper bound (dashed line) on the heavy W mass that is supplied by equation (3.23) in the absence of fine-tuned ETC interactions. No region of the plot satisfies both bounds, i.e. the model must be fine tuned in order to produce the top mass and agree with precision measurements. Allowing for the possibility of some fine tuning, the lowest possible heavy W mass at the 95% confidence level is roughly 1.6 TeV, for $0.7 < s^2 < 0.8$. This corresponds to $f > 2$ TeV, and hence a tuning of order

$$\frac{4M^2}{g^2 f^2} \approx 14\% \left(\frac{f_Q}{125\,\text{GeV}}\right)^3 \left(\frac{2\,\text{TeV}}{f}\right)^2 \left(\frac{175\,\text{GeV}}{m_t}\right). \tag{5.7}$$

A summary of the quality of the global fit to the precision electroweak data is given in Table 4. We conclude that the heavy case also gives a good fit to the data,

Model	χ^2	df	χ^2/df	probability
SM	33.8	22	1.53	5%
SM+S,T	32.8	20	1.64	4%
$\text{ETC}_{\text{heavy}}$	20.7	19	1.09	36%

Table 4: The best fits for the standard model, the standard model plus extra oblique corrections, and the non-commuting ETC model (heavy case). The inputs are $\alpha_s(M_Z) = 0.115$, and (for the ETC model) $s^2 = 0.97$.

but the masses of the new gauge boson are substantially heavier than in the light case.

The best fit values for the parameters (corresponding to Tables 1 and 4, i.e. the heavy case with $\alpha_s(M_Z) = 0.115$) are:

$$\begin{aligned} 1/x &= 0.0027 \pm 0.0093 \\ \delta g_L^b &= -0.0064 \pm 0.0074 \\ \delta g_L^\tau &= \delta g_L^{\nu_\tau} = -0.0024 \pm 0.0055 \ . \end{aligned} \tag{5.8}$$

6 Conclusions

Surprisingly we have found that both cases of the non-commuting ETC model can give a significantly better fit to experimental data than the standard model, even when one takes into account the fact that the ETC model has extra parameters that are fit to data. Part of this relative success of course is due to the fact that the standard model does not fit the data very well (contrary to current folklore), especially if $\alpha_s(M_Z) = 0.115$. One might object that the non-commuting ETC model is not an aesthetically pleasing model. Furthermore both the heavy and light cases required some fine-tuning. Nonetheless, our results provide a significant existence proof: there is at least one ETC model that can fit the precision electroweak data *better* than the standard model. The light case of this non-commuting ETC model is especially interesting since the heavy gauge bosons can be lighter than 1 TeV, and hence could potentially be directly produced at foreseeable accelerators.

Acknowledgments

J.T. thanks W. Marciano and W. Williams for helpful conversations regarding tau decays and statistics respectively. We thank K. Lane for comments on the manuscript.

R.S.C. acknowledges the support of an NSF Presidential Young Investigator Award, and a DOE Outstanding Junior Investigator Award. E.H.S. acknowledges the support of an NSF Faculty Early Career Development (CAREER) award. *This work was supported in part by the National Science Foundation under grants PHY-9057173 and PHY-9501249, and by the Department of Energy under grant DE-FG02-91ER40676.*

A Appendix: Equations for heavy case

The full list of corrections [8, 19] to standard model predictions in the 'heavy case' of non-commuting ETC is:

$$\begin{aligned}\Gamma_Z &= (\Gamma_Z)_{SM}\Big(1 - 0.707\delta g_L^b - 0.144\delta g_L^\tau + 0.268\delta g_L^{\nu_\tau} \\ &\quad + \Big(1.693 s^2c^2 - 0.559 s^4 - 1.350\left(1 - s^4\right)\Big)\frac{1}{x}\Big) \qquad \text{(A.1)}\end{aligned}$$

$$R_e = (R_e)_{SM}\left(1 - 1.01\delta g_L^b + \Big(-0.313 s^2c^2 - 0.505 s^4 - 0.260\left(1 - s^4\right)\Big)\frac{1}{x}\right) \qquad \text{(A.2)}$$

$$R_\mu = (R_\mu)_{SM}\left(1 - 1.01\delta g_L^b + \Big(-0.313 s^2c^2 - 0.505 s^4 - 0.260\left(1 - s^4\right)\Big)\frac{1}{x}\right) \qquad \text{(A.3)}$$

$$\begin{aligned}R_\tau &= (R_\tau)_{SM}\Big(1 - 1.01\delta g_L^b + 4.290\delta g_L^\tau \\ &\quad + \Big(1.832 s^2c^2 + 1.640 s^4 - 0.260\left(1 - s^4\right)\Big)\frac{1}{x}\Big) \qquad \text{(A.4)}\end{aligned}$$

$$\begin{aligned}\sigma_h &= (\sigma_h)_{SM}\Big(1 + 0.404\delta g_L^b + 0.288\delta g_L^\tau - 0.536\delta g_L^{\nu_\tau} \\ &\quad + \Big(0.591 s^2c^2 + 0.614 s^4 + 0.022\left(1 - s^4\right)\Big)\frac{1}{x}\Big) \qquad \text{(A.5)}\end{aligned}$$

$$R_b = (R_b)_{SM}\left(1 - 3.56\delta g_L^b + \Big(-1.832 s^2c^2 - 1.780 s^4 + 0.059\left(1 - s^4\right)\Big)\frac{1}{x}\right) \qquad \text{(A.6)}$$

$$A_{FB}^e = (A_{FB}^e)_{SM} + \Big(0.430 s^2c^2 - 0.614\left(1 - s^4\right)\Big)\frac{1}{x} \qquad \text{(A.7)}$$

$$A_{FB}^\mu = (A_{FB}^\mu)_{SM} + \Big(0.430 s^2c^2 - 0.614\left(1 - s^4\right)\Big)\frac{1}{x} \qquad \text{(A.8)}$$

$$A_{FB}^{\tau} = (A_{FB}^{\tau})_{SM} - 0.430\delta g_L^{\tau} + \left(0.215s^2c^2 - 0.215s^4 - 0.614\left(1-s^4\right)\right)\frac{1}{x} \quad \text{(A.9)}$$

$$A_{\tau}(P_{\tau}) = (A_{\tau}(P_{\tau}))_{SM} - 3.610\delta g_L^{\tau} + \left(-1.805s^4 - 2.574\left(1-s^4\right)\right)\frac{1}{x} \quad \text{(A.10)}$$

$$A_e(P_{\tau}) = (A_e(P_{\tau}))_{SM} + \left(1.805s^2c^2 - 2.574\left(1-s^4\right)\right)\frac{1}{x} \quad \text{(A.11)}$$

$$A_{FB}^{b} = \left(A_{FB}^{b}\right)_{SM} - 0.035\delta g_L^{b} + \left(1.269s^2c^2 - 0.017s^4 - 1.828\left(1-s^4\right)\right)\frac{1}{x} \quad \text{(A.12)}$$

$$A_{FB}^{c} = (A_{FB}^{c})_{SM} + \left(1.003s^2c^2 - 1.433\left(1-s^4\right)\right)\frac{1}{x} \quad \text{(A.13)}$$

$$A_{LR} = (A_{LR})_{SM} + \left(1.805s^2c^2 - 2.574\left(1-s^4\right)\right)\frac{1}{x} \quad \text{(A.14)}$$

$$M_W = (M_W)_{SM}\left(1 - 0.213\left(1-s^4\right)\frac{1}{x}\right) \quad \text{(A.15)}$$

$$M_W/M_Z = (M_W/M_Z)_{SM}\left(1 - 0.213\left(1-s^4\right)\frac{1}{x}\right) \quad \text{(A.16)}$$

$$g_L^2(\nu N \to \nu X) = \left(g_L^2(\nu N \to \nu X)\right)_{SM} - 0.244\left(1-s^4\right)\frac{1}{x} \quad \text{(A.17)}$$

$$g_R^2(\nu N \to \nu X) = \left(g_R^2(\nu N \to \nu X)\right)_{SM} + 0.085\left(1-s^4\right)\frac{1}{x} \quad \text{(A.18)}$$

$$g_{eA}(\nu e \to \nu e) = (g_{eA}(\nu e \to \nu e))_{SM} \quad \text{(A.19)}$$

$$g_{eV}(\nu e \to \nu e) = (g_{eV}(\nu e \to \nu e))_{SM} + 0.656\left(1-s^4\right)\frac{1}{x} \quad \text{(A.20)}$$

$$Q_W(Cs) = (Q_W(Cs))_{SM} + \left(-21.16\,c^2 + 1.450\left(1-s^4\right)\right)\frac{1}{x} \quad \text{(A.21)}$$

$$R_{\mu\tau} \equiv \frac{\Gamma(\tau \to \mu\nu\bar{\nu})}{\Gamma(\mu \to e\nu\bar{\nu})} = R_{\mu\tau}^{SM}(1 - \frac{2}{x}) \quad \text{(A.22)}$$

B Appendix: Equations for light case

We obtain the following corrections [19, 8] to standard model predictions in the light case of the non-commuting ETC models:

$$\begin{aligned}\Gamma_Z \;=\; (\Gamma_Z)_{SM}\Big(1 &- 0.707\delta g_L^{b} - 0.144\delta g_L^{\tau} + 0.268\delta g_L^{\nu_\tau} \\ &+ \left(-0.343c^4 + 0.559s^2c^2\right)\frac{1}{x}\Big)\end{aligned} \quad \text{(B.1)}$$

$$R_e = (R_e)_{SM}\left(1 - 1.01\delta g_L^{b} + \left(0.573c^4 + 0.505s^2c^2\right)\frac{1}{x}\right) \quad \text{(B.2)}$$

$$R_{\mu} = (R_{\mu})_{SM}\left(1 - 1.01\delta g_L^{b} + \left(0.573c^4 + 0.505s^2c^2\right)\frac{1}{x}\right) \quad \text{(B.3)}$$

$$R_\tau = (R_\tau)_{SM}\left(1 - 1.01\delta g_L^b + 4.29\delta g_L^\tau + \left(-1.572c^4 - 1.640s^2c^2\right)\frac{1}{x}\right) \tag{B.4}$$

$$\begin{aligned}\sigma_h &= (\sigma_h)_{SM}\left(1 + 0.404\delta g_L^b + 0.288\delta g_L^\tau - 0.536\delta g_L^{\nu_\tau}\right.\\ &\qquad \left. + \left(-0.613c^4 - 0.614s^2c^2\right)\frac{1}{x}\right)\end{aligned} \tag{B.5}$$

$$R_b = (R_b)_{SM}\left(1 - 3.56\delta g_L^b + \left(0.129c^4 + 1.780s^2c^2\right)\frac{1}{x}\right) \tag{B.6}$$

$$A_{FB}^e = (A_{FB}^e)_{SM} + 0.184c^4\frac{1}{x} \tag{B.7}$$

$$A_{FB}^\mu = (A_{FB}^\mu)_{SM} + 0.184c^4\frac{1}{x} \tag{B.8}$$

$$A_{FB}^\tau = (A_{FB}^\tau)_{SM} - 0.430\delta g_L^\tau + \left(0.399c^4 + 0.215s^2c^2\right)\frac{1}{x} \tag{B.9}$$

$$A_\tau(P_\tau) = (A_\tau(P_\tau))_{SM} - 3.610\delta g_L^\tau + \left(2.574c^4 + 1.805s^2c^2\right)\frac{1}{x} \tag{B.10}$$

$$A_e(P_\tau) = (A_e(P_\tau))_{SM} + 0.769c^4\frac{1}{x} \tag{B.11}$$

$$A_{FB}^b = \left(A_{FB}^b\right)_{SM} - 0.035\delta g_L^b + \left(0.520c^4 + 0.161s^2c^2\right)\frac{1}{x} \tag{B.12}$$

$$A_{FB}^c = (A_{FB}^c)_{SM} + 0.400c^4\frac{1}{x} \tag{B.13}$$

$$A_{LR} = (A_{LR})_{SM} + 0.769c^4\frac{1}{x} \tag{B.14}$$

$$M_W = (M_W)_{SM}\left(1 + 0.213c^4\frac{1}{x}\right) \tag{B.15}$$

$$M_W/M_Z = (M_W/M_Z)_{SM}\left(1 + 0.213c^4\frac{1}{x}\right) \tag{B.16}$$

$$g_L^2(\nu N \to \nu X) = \left(g_L^2(\nu N \to \nu X)\right)_{SM} - 0.529c^4\frac{1}{x} \tag{B.17}$$

$$g_R^2(\nu N \to \nu X) = \left(g_R^2(\nu N \to \nu X)\right)_{SM} + 0.850c^4\frac{1}{x} \tag{B.18}$$

$$g_{eA}(\nu e \to \nu e) = (g_{eA}(\nu e \to \nu e))_{SM} + 0.500c^4\frac{1}{x} \tag{B.19}$$

$$g_{eV}(\nu e \to \nu e) = (g_{eV}(\nu e \to \nu e))_{SM} - 0.156c^4\frac{1}{x} \tag{B.20}$$

$$Q_W(Cs) = (Q_W(Cs))_{SM} + 95.05c^4\frac{1}{x} \tag{B.21}$$

$$R_{\mu\tau} \equiv \frac{\Gamma(\tau \to \mu\nu\bar{\nu})}{\Gamma(\mu \to e\nu\bar{\nu})} = R_{\mu\tau}^{SM} \tag{B.22}$$

References

[1] P. Langacker, hep-ph/9408310; see also P. Langacker and J. Erler, http://www-pdg.lbl.gov/rpp/book/page1304.html, *Phys. Rev.* **D50** (1994) 1304.

[2] A.Blondel, http://alephwww.cern.ch/ALEPHGENERAL/reports/reports.html, CERN PPE/94-133.

[3] J. Erler and P. Langacker, hep-ph/9411203, UPR-0632-T.

[4] C.T.H. Davies et. al., hep-ph/9408328, OHSTPY-HEP-T-94-013, FSU-SCRI-94-79.

[5] I. Hinchliffe, http://www-pdg.lbl.gov/rpp/book/page1297.html, *Phys. Rev.* **D50** (1994) 1297; M. Virchaux, Saclay preprint, DAPHNIA/SPP 92-30, presented at the "QCD 20 years later" workshop, Aachen Germany, (1992); R. Voss, in *Proceedings of the 1993 International Symposium on Lepton and Photon Interactions at High Energies*, Ithaca NY (1993).

[6] B. Holdom, hep-ph/9407311, *Phys. Lett.* **B339** (1994) 114; T. Takeuchi, A.K. Grant and J.L. Rosner, hep-ph/9409211, Fermilab preprint FERMILAB-CONF-94/279-T; J. Erler and P. Langacker, hep-ph/9411203, U. of Pennsylvania preprint UPR-0632-T.

[7] S. Dimopoulos and L. Susskind, *Nucl. Phys.* **B155** (1979) 237; E. Eichten and K. Lane, *Phys. Lett.* **B90** (1980) 125.

[8] R.S. Chivukula, E.H. Simmons, and J. Terning, hep-ph/9404209, *Phys. Lett.* **B331** (1994) 383.

[9] A. Manohar and H. Georgi, *Nucl. Phys.* **B234** (1984) 189.

[10] R. S. Chivukula, K. Lane, and A. G. Cohen, *Nucl. Phys.* **B 343** (1990) 554; T. Appelquist, J. Terning, and L. Wijewardhana, *Phys. Rev* **44** (1991) 871.

[11] K. Lane and E. Eichten, *Phys. Lett.* **B222** (1989) 274.

[12] J. Terning, hep-ph/9410233, *Phys. Lett.* **B344** (1995) 279.

[13] C. Hill, *Phys. Lett.* **B345** (1995) 483.

[14] R.S. Chivukula, B.A. Dobrescu, and J. Terning, hep-ph/9503203.

[15] T. Appelquist and J. Terning, *Phys. Lett.* **B315** (1993) 139.

[16] T. Appelquist, M. Einhorn, T. Takeuchi, and L.C.R. Wijewardhana, *Phys. Lett.* **220B**, 223 (1989); V.A. Miransky and K. Yamawaki, *Mod. Phys. Lett.* **A4** (1989) 129; K. Matumoto *Prog. Theor. Phys. Lett.* **81** (1989) 277.

[17] H. Georgi, E.E. Jenkins, and E.H. Simmons *Phys. Rev. Lett.* **62** (1989) 2789, Erratum, ibid. **63** (1989) 1540 and *Nucl. Phys.* **B331** (1990) 541.

[18] R.S. Chivukula, E.H. Simmons, and J. Terning, hep-ph/9412309, *Phys. Lett.* **B346** (1995) 284.

[19] C.P. Burgess, et. al., hep-ph/9312291, *Phys. Rev.* **D49** (1994) 6115.

[20] T. Maskawa and H. Nakajima, Prog. Theor. Phys. **52** (1974) 1326 and **54** (1976) 860; R. Fukuda and T. Kugo, *Nucl. Phys.* **B117** (1976) 250; K. Higashijima, *Phys. Rev.* **D29** (1984) 1228; P. Castorina and S.Y. Pi, *Phys. Rev.* **D31** (1985) 411; R. Casalbuoni, S. De Curtis, D. Dominici, and R. Gatto, *Phys. Lett.* **B B150** (1985) 295; T. Banks and S. Raby, *Phys. Rev.* **D14** (1976) 2182; M. Peskin, in *Recent Advances in Field Theory and Statistical Mechanics*, Les Houches 1982, J.B. Zuber and R. Stora, eds., North-Holland, Amsterdam, 1984; A. Cohen and H. Georgi, *Nucl. Phys.* **B314** (1989) 7.

[21] Particle Data Group 1994; See also A. Pich and J.P. Silva hep-ph/95-5327, FTUV/95-21, IFIC/95-21.

[22] F. Abe et. al. (CDF collaboration), hep-ex/9503002; S. Abachi et. al. (D0 collaboration), hep-ex/9503003.

[23] M. Swartz, hep-ph/9411353, SLAC-PUB-6710; see also A.D. Martin and D. Zeppenfeld, hep-ph/9411377, MADPH-94-855; S. Eidelman and F. Jegerlehner, hep-ph/9502298, PSI-PR-95-1.

[24] B. Lynn, M. Peskin, and R. Stuart, in *Physics at LEP*, J. Ellis and R. Peccei eds. CERN preprint **86-02** (1986). M. Golden and L. Randall, *Nucl. Phys.* **B361**, 3 (1991); B. Holdom and J. Terning, *Phys. Lett* **B247**, 88 (1990); M. Peskin and T. Takeuchi, *Phys. Rev. Lett.* **65**, 964 (1990); A. Dobado, D. Espriu, and M. Herrero, *Phys. Lett.* **B253**, 161 (1991); M. Peskin and T. Takeuchi *Phys. Rev.* **D46** 381 (1992).

Figure Captions

Figure 1. The solid line is the 95% confidence lower bound for M_W^H as a function of s^2 for the light case (using $\alpha_s(M_Z) = 0.115$). The dotted line is the 68% confidence lower bound.

Figure 2. The 90% confidence region for ETC induced shifts in Z couplings for the light case (using $1/x = 0.028$ and $s^2 = 0.97$) for $\alpha_s(M_Z) = 0.115$ (solid line), and $\alpha_s(M_Z) = 0.124$ (dashed line). Note that the standard model prediction (the origin) is excluded for $\alpha_s(M_Z) = 0.115$.

Figure 3. The solid line is the 95% confidence lower bound for M_W^H as a function of s^2 for the heavy case (using $\alpha_s(M_Z) = 0.115$). The dotted line is the 68% confidence lower bound. The dashed line is the upper bound on M_W^H (in the absence of ETC fine-tuning). Note that there is no overlap region.

Figure 1

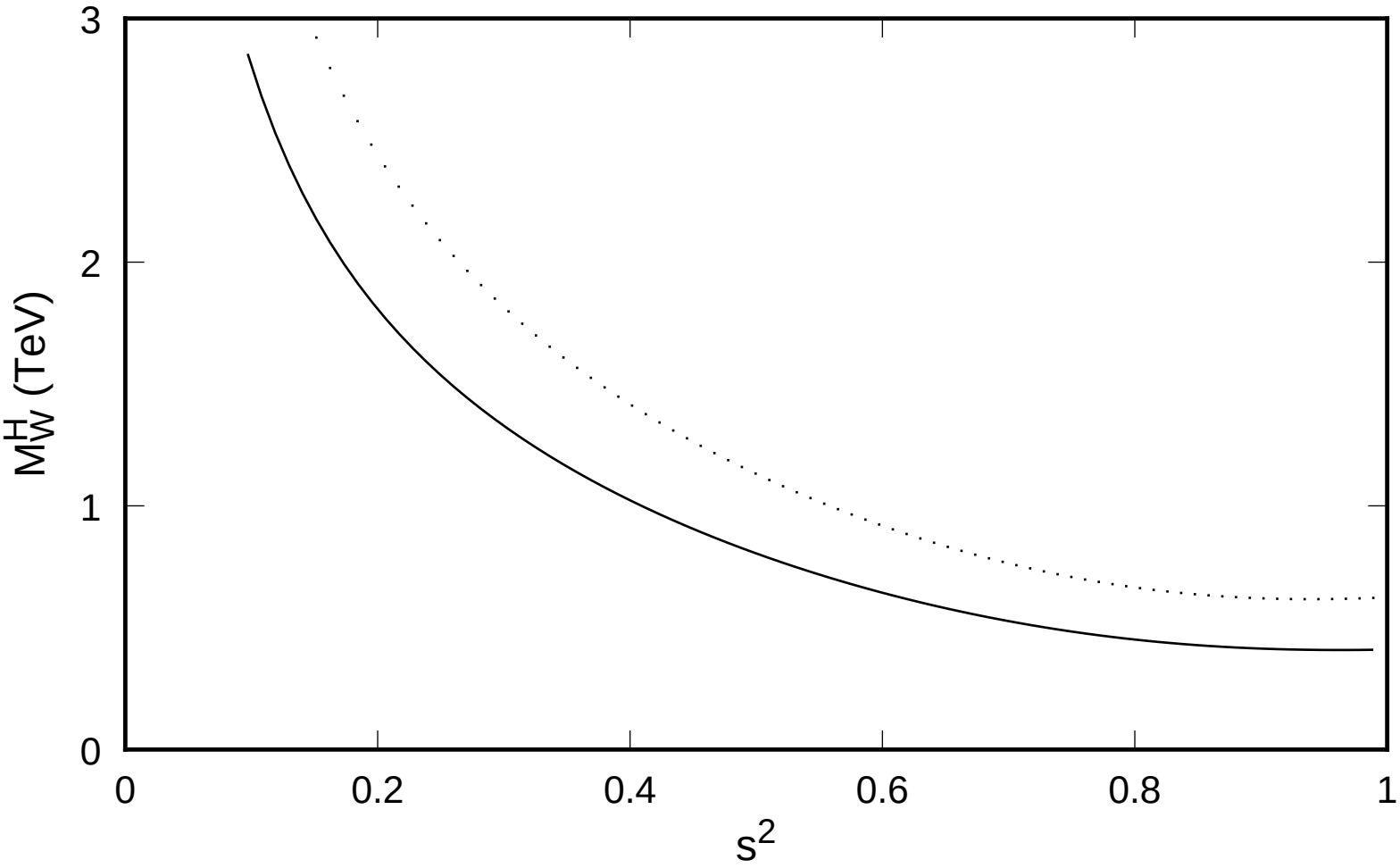

Figure 2

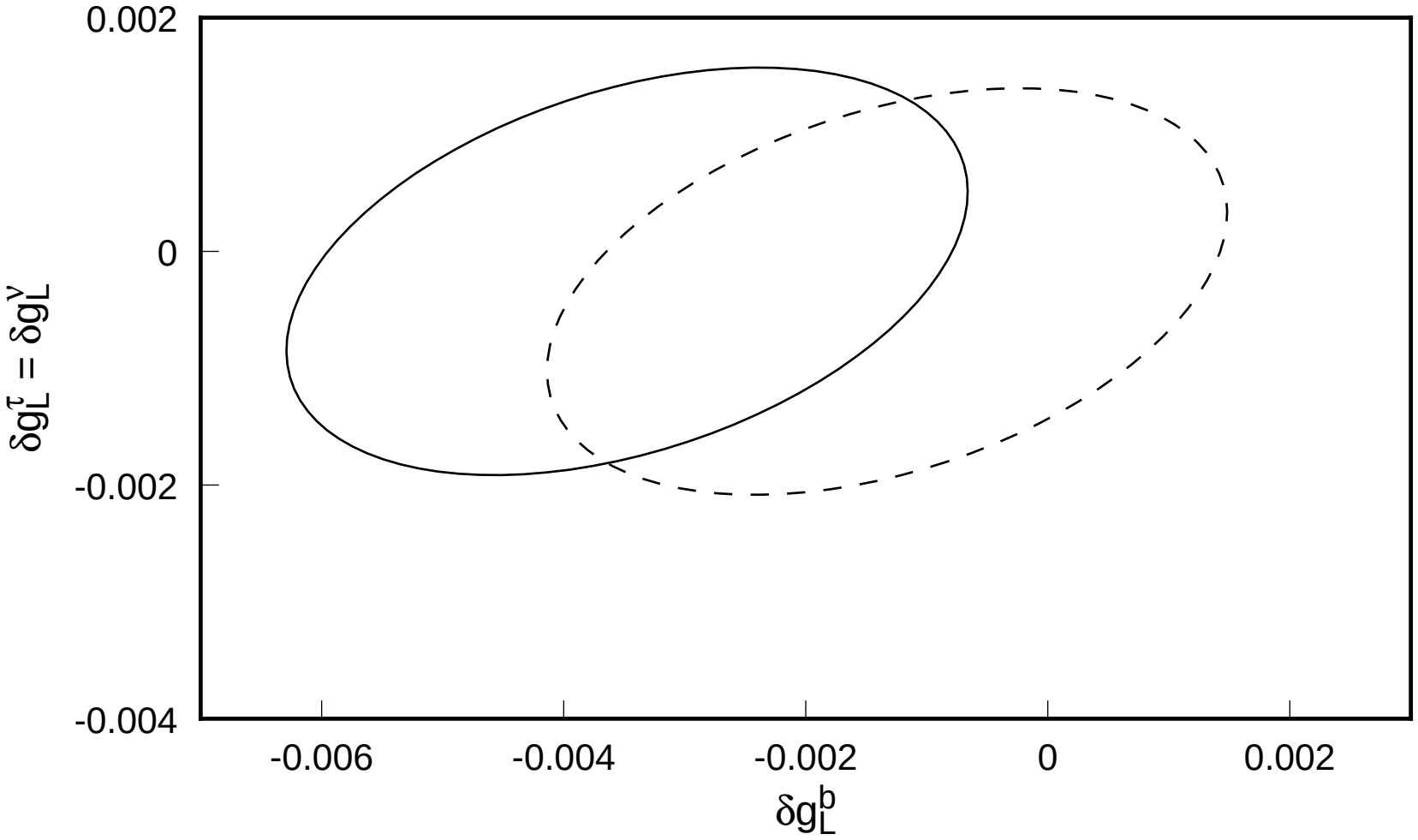
0.002
0
-0.002
-0.004
-0.006
-0.004
-0.002
0
0.002
$\delta g_L^\tau = \delta g_L^\nu$
δg_L^b

Figure 3